Research Article Vol. 1, No. 5 / 15 May 2022 / Optics Continuum 1060
OPTICS CONTINUUM

Enhancement of gain and efficiency of an Ho:YLF energy booster through deep thermoelectric cooling

FANGJIE ZHOU, ADRIAN CINTRON, YI WU, AND ZENGHU CHANG*

Institute for the Frontier of Attosecond Science and Technology, The College of Optics and Photonics (CREOL) and Department of Physics, University of Central Florida, Orlando, FL 32816, USA
**Zenghu.Chang@ucf.edu*

Abstract: It is well known that the gain and efficiency of an amplifier with a quasi-three level medium such as Ho:YLF is strongly affected by the coolant temperature. By cooling the Ho:YLF crystals of a two-stage energy booster in a Ho:YLF Chirped Pulse Amplification laser with -20°C thermoelectric cooling rather than room temperature water, a 60 mJ pulse energy at 1 kHz repetition rate was achieved with 8.5 mJ input.

1. Introduction

Many experiments of interest in strong-field physics require the production of long wavelength laser pulses [1–4]. Recent advancements in few-cycle, carrier-envelope phase locked, mJ-level short wavelength infrared (SWIR, 1.4-3 μm) lasers operating at 1 kHz or higher repletion rate have led to the development of attosecond X-ray sources in the water window (282 to 533 eV) [5]. High harmonic generation with spectrum cutoff beyond 1 keV has been demonstrated with mid-wave infrared (MWIR, 3-8 μm) driving lasers [6]. High peak-power (100-gigawatt-level) pulses within the 3.5-5 μm atmospheric transmission window are capable of forming filaments by self-focusing in air through the Kerr lens effect [7,8]; such pulses are ideal for defense applications, as they can reliably deliver maximum damage to a target with tremendous precision and minimal attenuation. Since gain media which operate in the MWIR wavelength region are limited, Optical Parametric Chirped Pulsed Amplification (OPCPA) stands out as an optimal method. Oxide nonlinear crystals such as Potassium Titanyle Arsenate (KTA) pumped by 1-μm lasers have enabled the generation of 30 mJ, 80 fs, 20 Hz pulses at 3.9 μm [9]. 2-μm pump sources double the fundamentally possible upper conversion efficiency and enable the use of non-oxide crystals such as $ZnGeP_2$ (ZGP) that has a much larger nonlinearity, $d_{36} = 75$ pm/V [10–12]. The thermal conductivity of ZGP is 36 W/(m·K), 20 times larger than that of KTA, and is critical for high repetition rate/high average power operation.

Ho:YLF enables the amplification of 2-μm picosecond pulses to tens of millijoules when pumped with 1.94 μm Tm:fiber lasers [13–15]. The $^5I_8$ and $^5I_7$ manifolds of Ho^{3+} contain 13 and 10 levels, respectively, as shown in Fig. 1 [16]. The amplification of pulses at 2.05 μm is due to the simulated emission transition between the upper laser level N_2 (at 5153 cm^{-1}) and the lower laser level N_1 (at 276 cm^{-1}). Ho:YLF is considered as a quasi-three level gain medium due to the small energy difference between the ground state N_0 (at 0 cm^{-1}) and the lower laser level. As seen in Fig. 1, the populations of the relevant laser levels change with temperature, consequently the gain of a quasi-three level amplifier like Ho:YLF depends strongly on temperature.

High energy picosecond Ho:YLF lasers are normally based on Chirped Pulse Amplification (CPA). In a 2-μm picosecond CPA laser that generates more than 20 mJ of energy, pulses from preamplifiers are boosted by power amplifiers. The final output energy is determined by the input pulse energy and the gain of the booster. Recently, a Ho:YLF CPA system that outputs 56 mJ using a regenerative amplifier and two-stages of booster amplification was demonstrated at

#456612 https://doi.org/10.1364/OPTCON.456612
Journal © 2022 Received 18 Feb 2022; revised 29 Mar 2022; accepted 30 Mar 2022; published 25 Apr 2022

OPTICS CONTINUUM

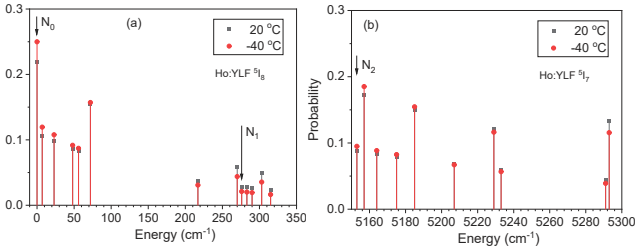

Fig. 1. Boltzmann fractions of the (a) $^5I_8$ and (b) $^5I_7$ levels of Ho:YLF at two temperatures, 20 °C and -40 °C. N_0, N_1, and N_2 are the ground state, lower, and upper laser levels, respectively, for amplifying signals at 2.05 µm.

1 kHz [13]. In this system, the crystals were water cooled with a coolant temperature of 8°C. The input energy to the booster amplifier was 12 mJ when pumped with 220 W total power and the single-pass gain of the booster amplifiers was 4.7. Additionally, the reported power conversion efficiency of the booster was 20%. Here, we report a two-stage Ho:YLF booster amplifier that utilizes two thermoelectric cooling modules (TECs) to achieve higher energy output by applying the temperature dependence of quasi-three level media. Under to operate, and less costly compared to cryogenic the same pumping power as that in [13], an output energy of 60 mJ was recorded for only 8.5 mJ input when the crystals were cooled to -20°C using TECs. To our knowledge, this is the highest output energy that has ever been produced from a tabletop kHz Ho:YLF amplifier. The corresponding gain and efficiency are 7 and 23.4% which, when combined with the fact that TECs are more compact, easier cooling [15], unequivocally show that using TECs is a superior way to enhance the performance of Ho:YLF amplifiers.

2. Experiment setup

The configuration of the Ho:YLF CPA is shown schematically in Fig. 2, which is similar to that reported in [14]. The 2.05 µm seed pulse is generated through a Dual-Chirped Optical Parametric Amplifier (DCOPA) driven by a femtosecond Ti:Sapphire CPA laser that produces 30 fs, 2 mJ pulses at 1 kHz [17]. 0.5% of the 800-nm pulse energy is focused onto a sapphire plate to generate a supercontinuum, and 1 mJ is used for pumping a 10-mm long BBO crystal. The same amount of dispersion is added to the signal and the pump, through a ZnSe and a SF57, to reduce the bandwidth of the idler pulses to 40 nm, centered at 2.05 µm. The 50 µJ idler pulse then propagates to a Chirped Volume Bragg Grating (CVBG) with 20×27 mm^2 aperture size, which serves as both the optical stretcher and the compressor. A quarter waveplate is place between the thin film polarizer and the stretcher to rotate the polarization of the reflected beam by 90 degree, so it can be reflected by the TFP and passed to the amplifier. The 4.5 nm bandwidth of the CVBG reduces the pulse energy to 5 µJ whilst stretching it to 470 ps. The seed energy is 4 orders of magnitude higher than that generated from Tm:fiber lasers used in [13] so that a multi-pass amplifier (rather than a regenerative amplifier, as in [13]) can be used to amplify the seed pulses to tens of millijoules while keeping the B-integral and high order dispersions small.

The first two stages of the amplifier employ a double-pass configuration. The stretched beam emerging from the CVBG is amplified inside two 0.75% doped, 5-mm diameter, 50-mm long cylindrical Ho:YLF crystals that share the same Tm:fiber pump. A Faraday rotator and a half wave plate are used in combination to rotate the polarization of the forward beam from the horizontal to the vertical while also keeping the backward beam vertically polarized to pass through the thin film polarizer. Both the emission and absorption cross sections of birefringent Ho:YLF depend strongly on the polarization; therefore, the unpolarized pump beam is divided in half by a polarizing beam splitter. The polarizations of both the pump and seed beams are parallel

OPTICS CONTINUUM

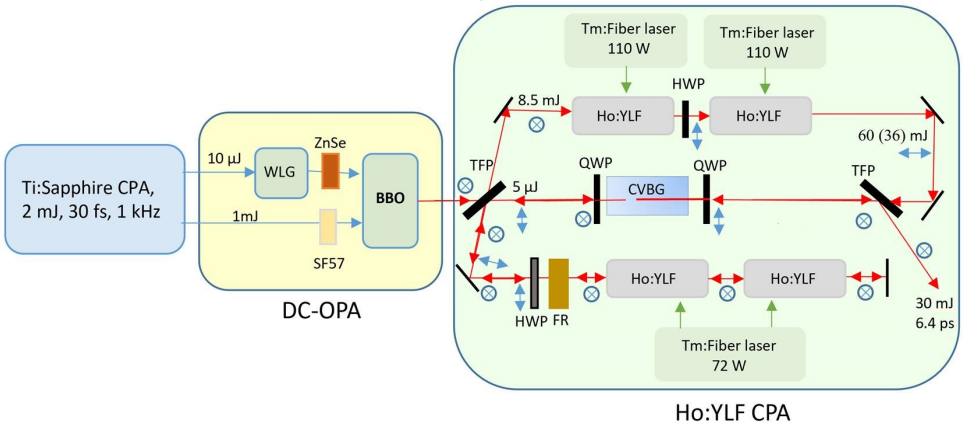

Fig. 2. Layout of the Ho:YLF CPA system. WLG (white light generation), QWP (Quarter wave plate), HWP (Half wave plate), TFP (Thin film polarizer), FR (Faraday rotator). 60 mJ pulses at 2.05 µm can be generated from the booster at 1 kHz and 36 mJ is compressed to 30 mJ.

to the c-axis of the crystals to maximize the gain, and the crystals are water cooled at 15°C. The output from the double passed amplifier was limited to 8.5 mJ at 72 W total pumping power, as any further amplification risked surpassing the damage threshold of the 4.5-mm aperture Faraday rotator. The improvement of the output energy as compared to our previous results in [14] was accomplished by increasing the pump and signal beam sizes in the two crystals.

The biggest difference between the current laser and the previous one [14] is the two single-pass booster amplifiers. The 0.75% doped, *a*-cut, 50-mm long crystals with an 8×8 mm^2 square aperture replaced the cylindrical crystals used in the past. The end faces were antireflection coated at the pump and signal wavelengths. Each crystal was cooled by a TEC module instead of a water chiller, which can dissipate 50 W of heat at -20°C when the TECs are themselves cooled by a water chiller at 5°C. The enclosure of the Ho:YLF laser is purged with dry nitrogen to a 0.1% relative humidity to reduce the dew point to -40°C, which prevents ice formation on the Ho:YLF crystals and mitigates the blooming effect of the Tm:fiber beam due to strong water vapor absorption. Each crystal was end-pumped by a 120 W Tm:fiber laser (not operating at their full power). The c-axes of the crystals for these two stages are orthogonal to balance their thermal lensing effect.

3. Discussion

The large population of the lower laser level (N_1) at room temperature leads to non-negligible absorption at the signal wavelength, 2.05 µm, which affects the performance of the booster amplifier. The temperature (T) and the space dependent gain coefficient can be calculated by

$$g(T, r, z) = \{\sigma_{em}(T)\beta(r, z) - \sigma_{ab}(T)[1 - \beta(r, z)]\}N_{tot}, \quad (1)$$

where z and r are the coordinates along and perpendicular to the propagation direction of the co-propagating pump and signal beams. $\beta(r, z)$ is the population inversion, which depends on the spatial distribution of the pump intensity. The Ho density $N_{tot} = 1.05 \times 10^{20} atoms/cm^3$ for 0.75% doping. The stimulated emission cross section σ_{em} and the absorption cross section σ_{ab} of Ho:YLF are 1.555×10^{-20} cm^2 and 0.502×10^{-20} cm^2, respectively, at 2.051 µm for π polarization at 27°C [18].

The spatial profile of the CW Tm:fiber laser can be modeled by a Gaussian function: $I_p(r) = I_0 e^{-4\ln(2)r^2/w^2}$. The 1/e^2 diameter of the pump beam at the input surface of the 3rd and

OPTICS CONTINUUM

4th stage amplifier crystals, $2w$ are 2.3 mm and 2.9 mm, respectively. The corresponding peak intensities (I_0) are 5295 and 3331 W/cm^2 when the crystals are pumped with 110 W power. The small signal gain at the transverse center is

$$G_{small}(T, r = 0) = e^{\int_0^L g(T,r=0,z)dz}. \tag{2}$$

As such, the absorption at the signal wavelength reduces the gain.

Unlike four-level gain materials, the absorption at the signal wavelength sets a threshold population inversion

$$\beta_{th}(T) = \frac{\sigma_{ab}(T)}{\sigma_{em}(T) + \sigma_{ab}(T)} \tag{3}$$

above which $g>0$. β_{th} (27°C) = 24.4%, requiring the pump intensity be higher than the saturation intensity (393 W/cm^2 at 27°C [18]). As a result, a large portion of the pump power transmits through the gain medium, limiting the efficiency of Ho:YLF amplifiers. The transmission of the 3rd and 4th stage with 110 W pumping power at 20°C are 51% and 33%, respectively. Reducing re-absorption of the signal by lowering the temperature of the crystal is beneficial for achieving high gain and high efficiency.

The calculated cross sections at the signal wavelength as a function of temperature are shown in Fig. 3. It is evident that the amplifier should be operated far below room temperature in order to increase σ_{em} and reduce σ_{ab}. When the crystals are cooled by TECs, the lowest temperature achievable is determined by their cooling power. By cooling each crystal with a TEC operating at 50% of its specified maximum power, a temperature of -20°C can be reached with 110 W pumping power.

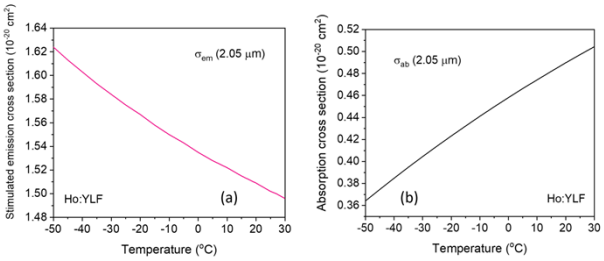

Fig. 3. Temperature dependence of the stimulated emission cross section and the absorption cross section σ_{ab} at the signal wavelength (2050nm).

The benefits of operating the Ho:YLF amplifier at very low crystal temperatures are confirmed by experiments. The measured transmission of the 1.5-mJ, 1 kHz signal at 2.05 μm from a preamplifier through the 3rd stage without pumping is shown in Fig. 4(a) and clearly demonstrates the effects of temperature on absorption. The small signal gain of a single amplifier (the 3rd stage, pumped with 110 W) measured with 2-mW CW input power from a diode laser as a function of temperature is shown in Fig. 4(b). The gain doubled (increased from 2 to 4) when the temperature was reduced from 15°C to -20°C.

To understand the dynamic upper-level electron density in the crystal, the relative intensity of the transmitted 3rd stage pump is measured using a fast oscilloscope and a photodiode, as shown in Fig. 4(e). The top to bottom difference of the transmitted pump intensity is normalized and indicates the relative density of the population inversion accumulated by the pump. An approximately 58% increase is observed at -20 °C compared to 15 °C. This result also implies a limit on the maximum pulse energy that can be achieved by reducing the repetition rate. The saturation of the pump can be observed at the moment when the seed is involved, indicating that the population inversion will not vary significantly when the spacing between pulses is longer.

OPTICS CONTINUUM

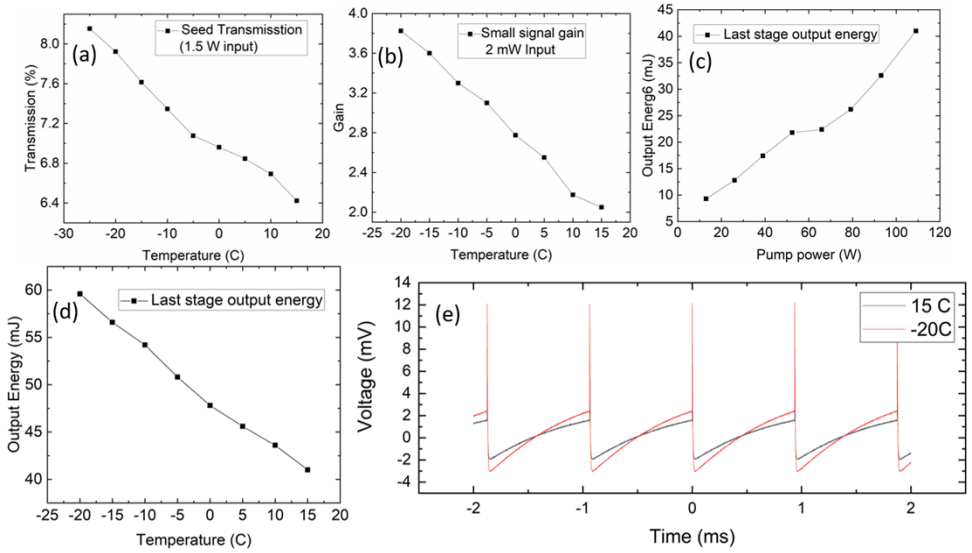

Fig. 4. (a) Small signal transmission at different temperatures measured at 1.5 mJ input power. (b) Small signal gain at different temperature measured at 2 mW input power. (c) Output energy of the two-stage booster with different pump powers at -20°C. (d) Output energy of the two-stage booster at different temperatures. (e) Time-resolved relative pump transmission. The sharp peak is the amplified seed.

The output energy of the laser pulse measured at the end of the 4th stage amplifier increased by a factor of ~1.5 (from 40 mJ to 60 mJ) for the 8.5 mJ input energy from the first two stages of the CPA when both the 3rd and 4th stages were pumped with 110 W. The gain of the single-pass two-stage booster is 7, which is much higher than that previously reported [13]. The high gain at -20°C allows a larger amplified signal beam diameter (1/e^2), 3 mm, in the final amplification stage and a lower fluence, 1.7 J/cm^2, thereby preventing laser-induced damage of the crystal faces. These results are especially promising, as they indicate that even higher output energies can be achieved by further reducing the crystal temperature, even if the pump power remains unchanged. In the laser setup used for this experiment, the crystal temperature is limited by the cooling power of the TECs for long term operation (75% of the specified maximum power as recommended by the manufacturer). Adding two more TECs to each cooling module is both feasible and will significantly reduce the crystal temperatures.

Each Tm:fiber laser used for pumping the 3rd and 4th stages can provide 120 W of power. The booster output as a function of the pump power of each stage is shown in Fig. 4(d). The output clearly increases monotonically with the pump without any sign of saturation; the change of the slope at ~60 W pump power is due to the shift of the wavelength of the Tm:fiber laser near the peak of a water vapor absorption line. The pump power used in the experiment was limited to 110 W to avoid damaging the Ho:YLF crystal by the amplified signal beam; however, the pump and signal beam size can be increased to make use of the full power of the Tm:fiber laser and obtain even higher output energies. The conversion efficiency from the total pump power, 220 W, to the net average power produced by the amplifier, 51.5W, is 23.4%. This value, which is crucial in directed energy applications where such lasers may be installed on airframes, surpasses the previous record of 20% [13]. Since the quantum efficiency of Ho:YLF is extremely high, 94.6%, there is tremendous room for improving the conversion efficiency by further lowering the crystal temperature. By applying 4 TEC modules to cool each booster amplifier crystal, -40 °C is

OPTICS CONTINUUM

reachable. The output energy is expected to be 70 mJ by extrapolating the results in Fig. 4(d). The corresponding conversion efficiency is 28%.

The M^2 of the output beam is estimated by the measured beam size (using Pyrocam III HR) at 10 points within the Rayleigh range and 10 points beyond two Rayleigh ranges. Due to the high thermo-optic coefficient dn/dT of Ho:YLF, the M^2 of the spatial profile increased from 1.5 to 1.9 as the pumping power was increased. The enhancement of the gain allows us to reach the same 36 mJ output energy that is reported in [14] with only 90 W of the pump power for both the 3rd and the 4th stage, reducing the beam distortion induced by the thermal lensing effect. The insert of Fig. 5 shows that the beam profile from the amplifier maintains a good beam quality, which is critical when pumping ZGP OPCPAs. The output of the booster is compressed to 6.4 ps by the same CVBG and in a same configuration that is used as the stretcher.

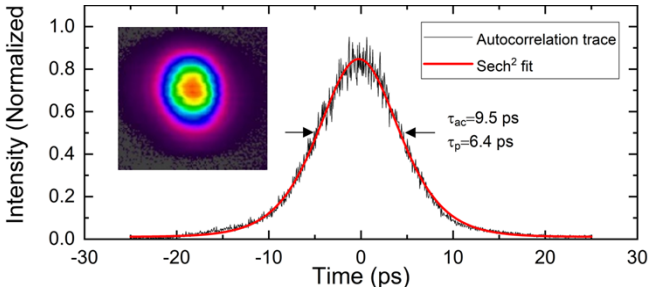

Fig. 5. The pulse duration when both pumps of the booster are at 90 W. Inset: Far field beam profile at the same pumping power.

4. Conclusion

We have demonstrated a novel and highly effective approach to enhance both the gain and efficiency of the two-stage energy booster in a Ho:YLF CPA system. By replacing water cooling with a TEC cooling system, the temperature of the crystal was reduced to -20°C, providing a 50% increase of the output energy. With just 8.5 mJ of input, a 60 mJ output was obtained, the highest gain and energy ever recorded from such boosters operating at a 1 kHz repetition rate, to the best of our knowledge. By adding more high power TEC cooling units to each booster module, it is expected that the Ho:YLF crystals can be cooled to even lower temperatures. As a result, the output energy and efficiency of the booster can be further increased, which is important for pumping high peak-power MWIR OPCPAs [10,11,19] and for directed energy applications.

Funding. Defense Threat Reduction Agency (HDTRA11910026); National Science Foundation – Directorate for Mathematical and Physical Sciences (1806575); Defense Advanced Research Projects Agency (D18AC00011); Air Force Office of Scientific Research (FA9550-20-1-0295).

Disclosures. The authors declare no conflicts of interest.

Data availability. Data underlying the results presented in this Letter are not publicly available at this time, but may be obtained from the authors upon reasonable request.

References

1. B. Shan and Z. Chang, "Dramatic extension of the high-order harmonic cutoff by using a long-wavelength driving field," Phys. Rev. A **65**(1), 011804 (2001).
2. J. Tate, T. Auguste, H. Muller, P. Salieres, P. Agostini, and L. DiMauro, "Scaling of wave-packet dynamics in an intense midinfrared field," Phys. Rev. Lett. **98**(1), 013901 (2007).
3. I. Pogorelsky, M. Babzien, I. Ben-Zvi, M. Polyanskiy, J. Skaritka, O. Tresca, N. Dover, Z. Najmudin, W. Lu, and N. Cook, "Extending laser plasma accelerators into the mid-IR spectral domain with a next-generation ultra-fast CO2 laser," Plasma Phys. Controlled Fusion **58**(3), 034003 (2016).

OPTICS CONTINUUM

4. S. Tochitsky, E. Welch, M. Polyanskiy, I. Pogorelsky, P. Panagiotopoulos, M. Kolesik, E. M. Wright, S. W. Koch, J. V. Moloney, and J. Pigeon, "Megafilament in air formed by self-guided terawatt long-wavelength infrared laser," Nat. Photonics **13**(1), 41–46 (2019).
5. X. Ren, J. Li, Y. Yin, K. Zhao, A. Chew, Y. Wang, S. Hu, Y. Cheng, E. Cunningham, and Y. Wu, "Attosecond light sources in the water window," J. Opt. **20**(2), 023001 (2018).
6. T. Popmintchev, M.-C. Chen, D. Popmintchev, P. Arpin, S. Brown, S. Ališauskas, G. Andriukaitis, T. Balčiunas, O. D. Mücke, and A. Pugzlys, "Bright coherent ultrahigh harmonics in the keV x-ray regime from mid-infrared femtosecond lasers," Science **336**(6086), 1287–1291 (2012).
7. A. Mitrofanov, A. Voronin, D. Sidorov-Biryukov, A. Pugžlys, E. Stepanov, G. Andriukaitis, T. Flöry, S. Ališauskas, A. Fedotov, and A. Baltuška, "Mid-infrared laser filaments in the atmosphere," Sci. Rep. **5**(1), 8368 (2015).
8. V. Shumakova, S. Ališauskas, P. Malevich, C. Gollner, A. Baltuška, D. Kartashov, A. Zheltikov, A. Mitrofanov, A. Voronin, and D. Sidorov-Biryukov, "Filamentation of mid-IR pulses in ambient air in the vicinity of molecular resonances," Opt. Lett. **43**(9), 2185–2188 (2018).
9. G. Andriukaitis, T. Balčiūnas, S. Ališauskas, A. Pugžlys, A. Baltuška, T. Popmintchev, M.-C. Chen, M. M. Murnane, and H. C. Kapteyn, "90 GW peak power few-cycle mid-infrared pulses from an optical parametric amplifier," Opt. Lett. **36**(15), 2755–2757 (2011).
10. Y. Yin, A. Chew, X. Ren, J. Li, Y. Wang, Y. Wu, and Z. Chang, "Towards terawatt sub-cycle long-wave infrared pulses via chirped optical parametric amplification and indirect pulse shaping," Sci. Rep. **7**(1), 45794 (2017).
11. L. von Grafenstein, M. Bock, D. Ueberschaer, E. Escoto, A. Koç, K. Zawilski, P. Schunemann, U. Griebner, and T. Elsaesser, "Multi-millijoule, few-cycle 5 µm OPCPA at 1 kHz repetition rate," Opt. Lett. **45**(21), 5998–6001 (2020).
12. U. Elu, T. Steinle, D. Sánchez, L. Maidment, K. Zawilski, P. Schunemann, U. Zeitner, C. Simon-Boisson, and J. Biegert, "Table-top high-energy 7 µm OPCPA and 260 mJ Ho: YLF pump laser," Opt. Lett. **44**(13), 3194–3197 (2019).
13. L. von Grafenstein, M. Bock, D. Ueberschaer, A. Koç, U. Griebner, and T. Elsaesser, "2.05 µm chirped pulse amplification system at a 1 kHz repetition rate—2.4 ps pulses with 17 GW peak power," Opt. Lett. **45**(14), 3836–3839 (2020).
14. K. Murari, F. Zhou, Y. Yin, Y. Wu, B. Weaver, T. Avni, E. Larsen, and Z. Chang, "Ho: YLF amplifier with Ti: Sapphire frontend for pumping mid-infrared optical parametric amplifier," Appl. Phys. Lett. **117**(14), 141102 (2020).
15. M. Hemmer, D. Sánchez, M. Jelínek, V. Smirnov, H. Jelinkova, V. Kubeček, and J. Biegert, "2-µm wavelength, high-energy Ho: YLF chirped-pulse amplifier for mid-infrared OPCPA," Opt. Lett. **40**(4), 451–454 (2015).
16. B. M. Walsh, "Spectroscopy and excitation dynamics of the trivalent lanthanides Tm3+ and Ho3+ in LiYF4," *NASA Contractor Rep*. 4689 (NASA Langley Research Center, Hampton, Va., 1995).
17. Y. Yin, X. Ren, Y. Wang, F. Zhuang, J. Li, and Z. Chang, "Generation of high-energy narrowband 2.05 µm pulses for seeding a Ho:YLF laser," Photonics Res. **6**(1), 1–5 (2018).
18. M. Schellhorn, "A comparison of resonantly pumped Ho: YLF and Ho: LLF lasers in CW and Q-switched operation under identical pump conditions," Appl. Phys. B **103**(4), 777–788 (2011).
19. D. Sanchez, M. Hemmer, M. Baudisch, S. Cousin, K. Zawilski, P. Schunemann, O. Chalus, C. Simon-Boisson, and J. Biegert, "7 µm, ultrafast, sub-millijoule-level mid-infrared optical parametric chirped pulse amplifier pumped at 2 µm," Optica **3**(2), 147–150 (2016).